SPANDIDOS PUBLICATIONS

ONCOLOGY LETTERS 2: 865-870, 2011

Evaluation of biodistribution and antitumor effects of ^{188}Re-rhk5 in a mouse model of lung cancer

RUI GUO[1], SHENG LIANG[1], YUFEI MA[2], HUA SHEN[2], HAOPING XU[1] and BIAO LI[1]

[1] Department of Nuclear Medicine, Ruijin Hospital, Shanghai Jiaotong University School of Medicine, Shanghai 200025; [2]Shanghai Institute of Applied Physics (SINAP), Chinese Academy of Sciences, Shanghai 201800, P.R. China

Received October 27, 2010; Accepted March 31, 2011

DOI: 10.3892/ol.2011.326

Abstract. Targeting drugs to receptors involved in tumor angiogenesis is considered to be a novel and promising approach to improve cancer treatment. This study aimed to evaluate the anti-tumor efficacy of ^{188}Re-labeled recombinant human plasminogen kringle 5 (^{188}Re-rhk5) through [^{18}F]-fluorodeoxyglucose (FDG) micro-positron emission tomography (PET). Radiolabeled rhk5 was obtained by conjugating the hystidine (6 x His) group at the carbon end of rhk5 with fac-[^{188}Re$(H_2O)_3(CO)_3]^+$. The biodistribution study of ^{188}Re-rhk5 showed that ^{188}Re-rhk5 had a high initial tumor uptake and prolonged tumor retention. The highest tumor uptake of ^{188}Re-rhk5 (3.65±0.82% ID/g) was found 2 h after injection which decreased to 0.81±0.14% ID/g 12 h after injection. Following therapy, tumor size measurement indicated that ^{188}Re-rhk5-treated tumors were smaller than ^{188}Re-, rhk5- and saline-treated controls 6 days after the treatment. *In vivo* ^{18}F-FDG micro-PET imaging showed significantly reduced tumor metabolism in the ^{188}Re-rhk5-treated mice vs. those treated with rhk5, ^{188}Re and saline control, 1 day after treatment. Moreover, the number of microvessels was significantly reduced after ^{188}Re-rhk5 treatment as determined by CD31 staining. Our results demonstrate that specific delivery of ^{188}Re-rhk5 allows preferential cytotoxicity to A549 lung cancer cells and tumor vasculature. ^{18}F-FDG micro-PET is a non-invasive imaging tool that can be utilized to assess early tumor responses to ^{188}Re-rhk5 therapy.

Introduction

Angiogenesis plays an important role in the process of tumor proliferation and migration. Intervention in any one of these processes affects angiogenesis and, consequently, inhibits tumor growth (1). Kringle 5 (k5), an internal proteolytic fragment of plasminogen, is an inhibitor of angiogenesis. It has a low molecular weight protein (14 kDa), with low immunocompetence, which has the most potent anti-angiogenic effect compared to other kringle fragments of plasminogen, including widely used angiostatin (2). However, a high dosage of inhibitor is required for tumor treatment, and these doses are not cost-effective for clinical application. By combining well-selected radionuclides with disease-specific drugs, the administration of radiolabeled drugs provides a functional imaging and efficient internal radiotherapy mode for localized as well as metastatic lesions (3,4).

Although ^{131}I is a widespread radioisotope used for tumor imaging and therapy, the use of ^{188}Re from the ^{188}W/^{188}Re-generator system is an attractive alternative radionuclide. ^{188}Re has a physical half-life of 16.9 h and, in addition to the emission of high-energy electrons (E_β=2.118 MeV), ^{188}Re also decays with emission of a γ-photon with an energy of 155 keV. Apart from the therapeutic usefulness of ^{188}Re, the biodistribution of ^{188}Re-labeled proteins can be evaluated *in vivo*. Since lung cancer is the most common cause of cancer-related mortality, the role of angiogenesis is well established in the progression of lung cancer (5). Consequently, ^{188}Re-labeled recombinant human plasminogen kringle 5 (^{188}Re-rhk5) radiotherapy was assessed in the experimental mouse models of lung cancer.

Methods that reliably evaluate and predict anti-tumor effects following therapy are currently rare. The ability to predict which type of therapy is effective at the early stage of treatment would be invaluable for drug selection. Conventional anatomic imaging modalities, such as computed tomography and endoscopic ultrasonography, reveal the cancer response as changes in tumor size and composition, which may occur only after weeks or months after therapy, and are not ideally suitable for the early prediction of tumor response (6). Positron emission tomography (PET) with the glucose analogue [^{18}F]-fluorodeoxyglucose (FDG) is a method utilized to monitor treatment responses (7). Thus, we evaluated the anti-tumor efficacy of ^{188}Re-rhk5 using ^{18}F-FDG micro-PET.

Materials and methods

General. Rhk5 was expressed as previously described with some modifications (8). The hystidine (6 x His) group was expressed at the carbon end of rhk5 for the purpose of ^{188}Re

Correspondence to: Professor Biao Li, Department of Nuclear Medicine, Ruijin Hospital, Shanghai Jiaotong University School of Medicine, Shanghai 200025, P.R. China
E-mail: lb10363@rjh.com.cn

Key words: ^{188}Re, kringle 5, tumor therapy, imaging, micro-positron emission tomography, [^{18}F]-fluorodeoxyglucose

labeling. All reagents, unless otherwise specified, were of analytical grade and purchased commercially. The borane ammonia complex (90% technical purity) was purchased from Sigma-Aldrich; (St. Louis, MO, USA). Carbon monoxide (CO) was obtained from Kunshan XinAn Industry Gas Co. Ltd. (Kunshan, China). SiL GF254 glass plate was purchased from Si-qing Biochemical Material Factory (Taizhou, China). ^{188}Re-perrhenate was eluted from a ^{188}W/^{188}Re generator (Radiopharmaceutical Centre, Shanghai Institute of Applied Physics, Shanghai, China) using 0.9% saline. A PD-10 column was purchased from GE Healthcare (Amersham Biosciences Corp., Piscataway, NJ, USA). Thin-layer chromatography (TLC) analysis was performed using silica gel 60 GF254 plates on a Bioscan system AR-2000 (Bioscan Inc., Washington DC, USA) with Winscan software, version 3.09. Radioactive samples from *in vivo* experiments were measured using a gamma-counter (SN-697; Shanghai Rihuan Photoelectronic Instrument Co. Ltd., Shanghai, China). ^{18}F-FDG was purchased from Shanghai Kexin Co. Ltd. and the micro-PET/CT system was from Siemens (Inveon; Siemens Medical Solutions, Knoxville, TN, USA). CD31 monoclonal antibodies were purchased from NeoMarkers (Fremont, CA, USA).

Preparation of fac-[Re(CO)$_3$(H$_2$O)$_3$]$^+$ and the radiolabeling of rhk5. The carbonyl complex fac-[Re(CO)$_3$(H$_2$O)^3]$^+$ was prepared by a previously described method (9,10), with some modifications. Radiolabeling of rhk5 was performed by a previously described method with some modifications (11). Briefly, powdered BH_3-NH_3 (5 mg) was placed into a 10-ml glass vial. The vial was sealed and flushed with CO for 20 min, and a mixture of 6 μl phosphoric acid (85%) and 1 ml of perrhenate (740-1110 MBq) was added to the vial. The vial was then heated in a water bath at 75˚C for 15 min. rhk5 solution (50 μg) was mixed with 1 ml of freshly prepared fac-[^{188}Re(CO)$_3$(H$_2$O)$_3$]$^+$ and incubated at 50˚C for 30 min. The radiolabeling efficiency was determined by TLC and purified by a PD-10 column.

Animal model. Female 5-week-old athymic Balb/c nude mice were used. Three mice were included in each group. The study was performed under intraperitoneally (i.p.) injected anesthesia (3% pentobarbital, 0.1 ml). A xenograft model was generated by subcutaneous injection of viable A549 cells (5x10^6 cells, suspended in 150 μl PBS) into the right hind limbs of the mice. Approximately 3 weeks after inoculation, with a tumor diameter of 0.6-0.8 cm, the mice were used for subsequent experiments. The animal experiments were performed in accordance with the EC directive 86/609/EEC for animal experiments.

Tissue biodistribution of ^{188}Re-rhk5. A total of 25 A549 tumor-bearing Balb/C nude mice were anesthetized by an i.p. injection of pentobarbital sodium (150 mg/kg). The mice were randomly divided into 5 groups (n=5 per group). Each animal received a 0.74 MBq intravenous (i.v.) injection of ^{188}Re-rhk5 to evaluate the biodistribution of the tracer in the major organs. Five of the mice were sacrificed at 0.5, 1, 2, 4 and 12 h after injection of ^{188}Re-rhk5, respectively. The principal organs, as well as blood and muscle samples, were removed and collected, washed with saline, weighed and counted using the gamma-counter. Tissue counts were corrected for background and decay during the time of counting. The results were presented as the percentage of the injected dose per gram of net weight (% ID/g). Each value is the mean ± SD of 5 animals.

In order to verify the binding specificity of ^{188}Re-rhk5, a blocking experiment was performed. In the blocking group, 5 tumor-bearing nude mice were used and each animal was administered 0.74 MBq ^{188}Re-rhk5 along with 100 μg rhk5. The animals were then presented for the biodistribution study 2 h post-injection, using the same procedure as above. The biodistribution data between the two groups were compared.

Treatment of A549 lung cancer model. A total of 24 mice were used. When palpable tumors were present in all animals (200-300 mm^3), the mice were randomly divided into 4 groups (n=6 per group). Group 1 was treated with ^{188}Re-rhk5 (37 MBq). As controls, Groups 2, 3 and 4 were treated with ^{188}Re (37 MBq), rhk5 (5 μg) and 0.9% saline, respectively. Considering the therapeutic efficacy and renal toxicity, the agents were injected directly into the tumor site. The tumor volume was measured every 3 days up to 18 days before euthanasia.

Measurement of tumor size. Tumor growth was assessed by caliper measures of the tumors the day before treatment, and every 3 days for 18 days following treatment. The tumor volume was estimated by the formula: Tumor volume = α x (b^2)/2, where α and b are the tumor length and width, respectively, in millimeters. The mice were sacrificed 18 days later.

Micro-PET/CT imaging. In the model, progression of the A549 xenografted tumors was determined by imaging mice treated with ^{188}Re-rhk5 at different time points (prior to ^{188}Re-rhk5 treatment and after 1, 6 and 18 days). Mice were sacrificed following completion of the last imaging, and histological assessment was performed to correlate tumor progression with micro-PET results.

After 8 h of fasting, CT images were initially obtained. The X-ray voltage was set at 80 kV, with a current of 500 μA. The total CT scan time was 10 min. The PET data were obtained at the same anatomic locations. Mice were injected with ~7.4 MBq of ^{18}F-FDG via tail vein under isoflurane anesthesia. The mice received 5% isoflurane in oxygen during rapid inhalation induction anesthesia (1-2 min). Maintenance of anesthesia during each scan was achieved using 1.5% isoflurane in oxygen. PET scans (20-min) were performed at 1 h post-injection (p.i.). The images were reconstructed by a three-dimensional ordered subset expectation maximum algorithm. All corrections for attenuation, scatter, dead time and randoms were applied to generate quantifiable images. The plane in which the tumor appeared largest on the CT image was selected. An irregular region of interest covering the whole tumor on CT was drawn and then copied to PET in the same mirror image. The maximum standardized uptake values (SUVmax) were determined.

Histopathological and immunohistochemical analysis. The mice were sacrificed using an overdose of pentobarbitone. Tumors were harvested in 4% buffered formaldehyde for 24 h, processed in paraffin, sectioned at 3 μm and stained with hematoxylin and eosin for histopathological examination.

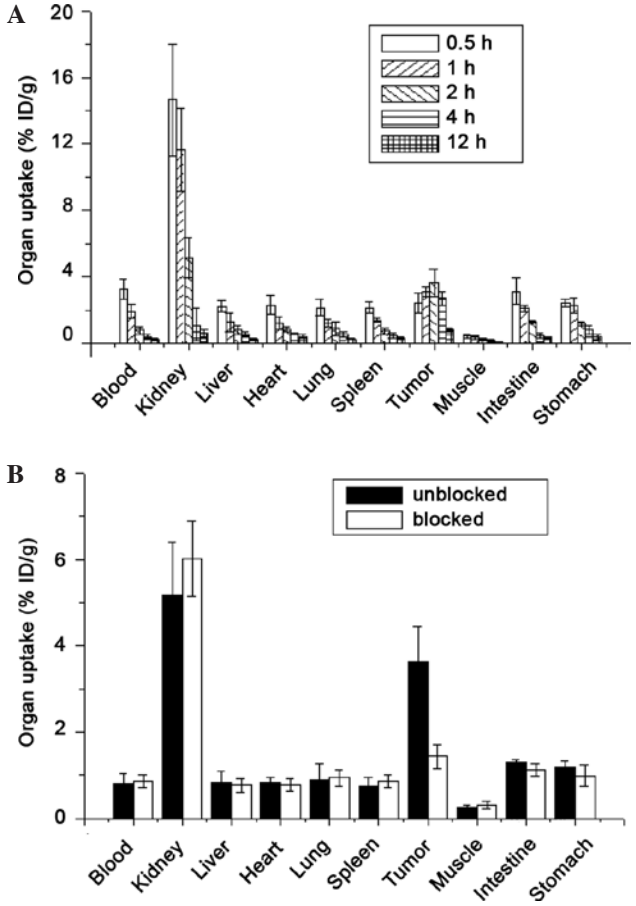

Figure 1. Tumor biodistribution study before and after blocking with rhk5. (A) Biodistribution of ^{188}Re-rhk5 in nude mice bearing subcutaneously xenotransplanted A549 tumors. (B) Tumor biodistribution study after blocking with rhk5. Tumor biodistribution percentage of injected dose per gram (% ID/g) of ^{188}Re-rhk5, with or without rhk5 (100 μg per mouse) blocking 2 h post-injection (0.74 MBq). Data are reported as the mean ± SD (n=5).

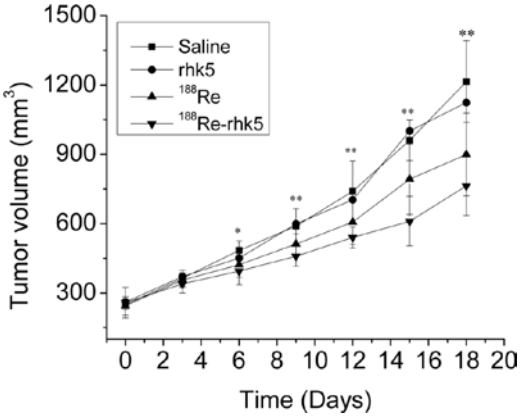

Figure 2. Therapeutic effects of ^{188}Re-rhk5 in tumor models measured by the change in tumor volume. Changes in tumor volume of ^{188}Re-rhk5 (37 MBq), ^{188}Re (37 MBq), rhk5 (5 μg) and 0.9% saline-treated tumors at various endpoints. The average tumor size was monitored every 3 days and is shown as the mean ± SD (n=6). *P<0.05 and **P<0.01.

For immunoreactivity staining, 5-μm deparaffinized polysin-coated sections were treated with 3% hydrogen peroxide for non-specific binding. A CD31 antibody (with a dilution of 1:200) was employed for immunohistochemical staining using the peroxidase-antiperoxidase technique.

Statistical analysis. Statistical significance was determined by one-way ANOVA using the Computer Statistical Package for the Social Sciences (SPSS 16.0). P<0.05 was considered to be statistically significant.

Results

Labeling of rhk5. TLC, using a SiL GF254 glass plate as the stationary phase and CH_3OH:HCl (36% in concentration) (99:1) as the mobile phase showed that the chelating efficacy of fac-[^{188}Re$(CO)_3(H_2O)_3$]$^+$ was >95%. $^{188}ReO_2$ and $^{188}ReO_4$ are rare. The radiolabeled efficacy of ^{188}Re-rhk5 was 60-75% after purification, and RCP was >96%. Therefore, ^{188}Re-rhk5 was adequately prepared, with a concentration of 280-390 MBq/ml, and was ready for the experiments.

Biodistribution study. Fig. 1A shows the biodistribution data at 0.5, 1, 2, 4 and 12 h post-injection. The radiotracer exhibited a rapid decrease in radioactivity over time in blood and the majority of organs. At early time points, the high kidney activity was evidently attributable to the elimination of ^{188}Re-rhk5 in the urine. The highest tumor uptake of ^{188}Re-rhk5 (3.65±0.82% ID/g) was found 2 h after injection and decreased to 0.81±0.14% ID/g 12 h after injection, suggesting that the ^{188}Re-rhk5 was present in the tumor up to at least 12 h after injection.

When blocked by a co-injection of rhk5 at a dose of 100 μg per mouse, the tumor uptake decreased from 3.65±0.82 to 1.44±0.28% ID/g for the A549 tumors 2 h after injection. Blocking reduced the tumor uptake of the tracer, clearly indicating specific binding. In contrast, co-injection of a large excess of rhk5 resulted in no change in the uptake of ^{188}Re-rhk5 in the remaining organs (Fig. 1B). The findings suggest that the tumor uptake of ^{188}Re-rhk5 occurs via a receptor-mediated process.

Changes in tumor volume following ^{188}Re-rhk5 treatment. To determine whether ^{188}Re-rhk5 has an anti-tumor effect *in vivo* as we proposed, female athymic nude mice-bearing A549 tumors were randomly divided into 4 groups and i.v. injected once with ^{188}Re-rhk5 (37 MBq), ^{188}Re (37 MBq), rhk5 (5 μg) and 0.9% saline. Prior to therapy, no significant difference was found in the tumor volume among the 4 groups (Fig. 2). The tumor volume in the 4 groups increased gradually on day 3, but no significant differences were noted among the groups at these time points (P>0.05). ^{188}Re-rhk5-treated tumors started to show growth retardation as compared to the 0.9% saline-treated group (P<0.05) at day 6 after initiation of treatment. The ^{188}Re group also showed a decrease in tumor growth compared to the 0.9% saline-treated group (P<0.05). However, no difference was found between the ^{188}Re- and ^{188}Re-rhk5-treated groups on day 6. It was found that 18 days after therapy the tumor volume was significantly smaller in the ^{188}Re-rhk5-treated group than in the controls (P<0.01).

^{18}F-FDG micro-PET imaging. ^{18}F-FDG micro-PET is a functional imaging technique that expresses the glycolytic rate of tissues and has been used to measure the increased metabolic

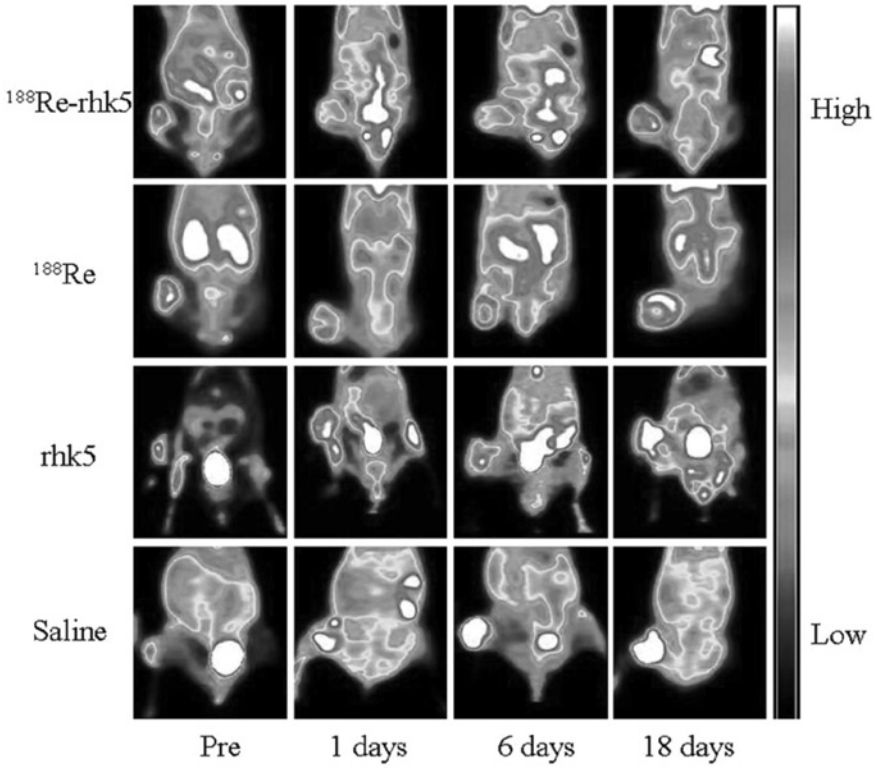

Figure 3. ^{18}F-FDG micro-PET imaging. Representative coronal micro-PET images of A549 tumor-bearing mice with ^{18}F-FDG prior to therapy and at 1, 6 and 18 days following therapy. The first row of images shows ^{188}Re-rhk5-induced tumor metabolic activity by micro-PET imaging following a single dose of administration of approximately 200 μCi of ^{18}F-FDG. The following 3 rows of images show ^{188}Re, rhk5 and saline-induced tumor metabolic activity. Implanted tumors are located on the right hind limbs of mice. Color scale, high (white) and low (black) radiotracer uptake.

demand in tumor cells. Currently, PET is used in both the evaluation and prediction of tumor response early during the course of therapy.

The accumulation of ^{18}F-FDG in tumor lesions prior to therapy was evident (Fig. 3). On day 1, a decrease in the ^{18}F-FDG uptake was evident in the ^{188}Re-rhk5 group. Uptake was also decreased in the ^{188}Re group, but not in the 2 control groups, which showed signs of increase. Changes in tumor size were a late sign; only at day 6 was there a distinction among the groups (Fig. 2). Due to the rapid proliferation and invasiveness of the malignant tumors, a single dose of ^{188}Re-rhk5 did not eliminate all viable tumor cells. The remaining tumor cells proliferated rapidly; ^{18}F-FDG uptake increased following a rapid decrease after ^{188}Re-rhk5 treatment. On day 18, ^{18}F-FDG uptake of all the control groups was increased, while the uptake of the ^{188}Re-rhk5-treated group remained less than that of the control groups.

The tumor uptake of ^{18}F-FDG (SUVmax) was decreased from 0.72±0.18 to 0.31±0.08% ID/g in the ^{188}Re-rhk5-treated group (P<0.01), and from 0.74±0.10 to 0.50±0.08% ID/g in the ^{188}Re-treated group (P<0.01) (Fig. 4). Both rhk5- and saline-treated groups exhibited no change in SUVmax. After day 6, both ^{188}Re-rhk5- and ^{188}Re-treated groups showed a low level of SUVmax similar to that on day 1. However, the remaining two groups showed an increased SUVmax. The SUVmax of the ^{188}Re-rhk5-treated group was lower than that at pre-therapy, even 18 days after therapy. However, the remaining 3 groups reached a higher level of SUVmax than that at pre-treatment.

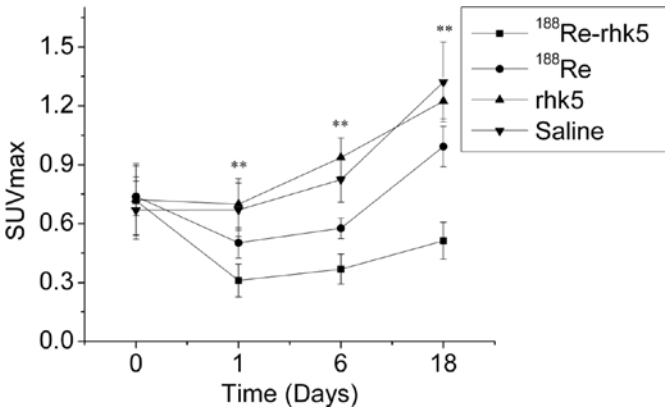

Figure 4. Changes in the ^{18}F-FDG uptake following ^{188}Re-rhk5 treatment. A comparison of the uptake of ^{18}F-FDG in A549 tumors treated with ^{188}Re-rhk5 (37 MBq), ^{188}Re (37 MBq), rhk5 (5 μg) and 0.9% saline at various time points (0, 3, 6 and 18 days) is shown. ^{18}F-FDG micro-PET was performed 1 h after injection with 200 μCi ^{18}F-FDG. Implanted tumors are located on the right hind limbs of mice. SUVmax was calculated.

Histological analysis. To further confirm the effectiveness of the use of ^{188}Re-rhk5 treatment, we performed a histological analysis on the dissected tumors (Fig. 5). Mice treated with ^{188}Re-rhk5 showed a marked necrosis compared to the other 3 groups. CD31 staining was carried out to study the effect of ^{188}Re-rhk5 treatment on vascular damage. It was found that CD31 expression was decreased in the ^{188}Re-rhk5 group when compared to the ^{188}Re, rhk5 and saline groups. Therefore, by combining the use of bioimaging techniques as well as histo-

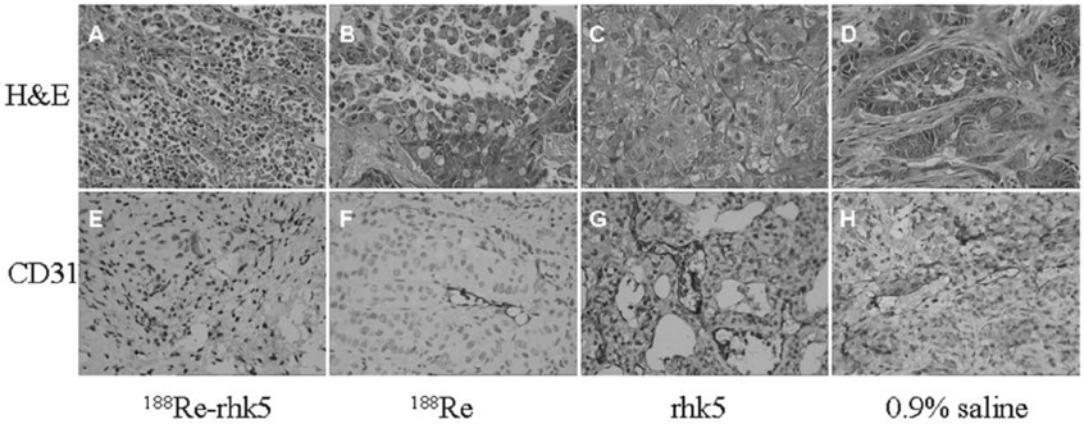

Figure 5. Histological and immunohistochemical analysis following therapy. Histological and CD31 immunohistochemical analysis of the effects of ^{188}Re-rhk5, ^{188}Re, rhk5 and 0.9% saline on A549 xenografts. All of the tests were performed 18 days after treatment. Representative histological sections (A-D) and CD31 immunohistochemical analysis (E-H) for A549 xenografts (magnification, x40).

logical analysis, we demonstrated that ^{188}Re-rhk5 therapy is effective against A549 xenografts in a mouse model.

Discussion

The development of successful tumor imaging and radiopharmaceutical therapy requires a detailed understanding of the target molecules. Consequently, the targets for rhk5 on endothelial cells have been studied. It is known that rhk5 specifically binds to endothelial cell surface ATP synthase (12). The present biodistribution and blocking study confirmed the specificity of rhk5 binding.

Radioimmunotherapy of tumors using molecules labeled with β-emitters has been proposed as part of a combined modality approach in order to improve the prognosis of patients (13,14). Positive clinical responses have been achieved by a number of investigators (15,16). The systemic administration of radiopharmaceuticals for therapeutic purposes is limited by various factors, such as high interstitial pressure inside the neoplastic tissue, limited blood supply to the tumor, inhomogeneous and inconsistent antigen expression, possible presence of histopathological barriers (necrosis or fibrosis) and catabolism of immunoglobulins (17). These factors result in a very low accumulation of the radiopharmaceutical in the target tissue, which in most cases prevents a favorable therapeutic effect.

In the present study, by targeting neovessels, the tumor specificity of rhk5 and cytotoxic effect of ^{188}Re were observed. We evaluated the tumor therapeutic effect of ^{188}Re-rhk5 *in vivo*, with ^{188}Re, rhk5 and saline-only treatment serving as controls. In subsequent experiments, the tumor response to therapy was confirmed by tumor volume measurement, ^{18}F-FDG PET and *in vitro* histopathological validation.

Following the measurement of tumor size, mice treated with ^{188}Re-rhk5 exhibited a slower tumor growth than ^{188}Re-, rhk5- and saline-treated controls. ^{188}Re treatment also exhibited a delay in tumor growth when compared to the rhk5 treatment group and saline controls. ^{18}F-FDG PET revealed a reduced tumor metabolism following ^{188}Re-rhk5 and ^{188}Re treatment, which concurred with the observation that ^{188}Re-rhk5 and ^{188}Re decreased the rate of tumor growth; although the tumor volume still increased with time despite the ^{188}Re-rhk5 administrations. This study showed that ^{18}F-FDG PET was suitable for depicting early glycolytic rate reductions in A549 tumors (1 day after therapy) in pre-clinical models following ^{188}Re-rhk5 therapy before changes in tumor size were evident. Further studies are required to determine whether ^{18}F-FDG PET distinguishes between varying degrees of treatment response, predicts a pathologic complete response, and detects early biological changes during the regrowth phase following ineffective therapy. Results of *in vitro* immunohistochemistry revealed that ^{188}Re-rhk5 is more effective than ^{188}Re or rhk5 in terms of eradicating tumor vasculature. Further studies to evaluate the effect of various doses and treatment frequencies are required to optimize treatment efficacy.

Our study is novel in that it compared the diagnostic values of micro-PET/CT and conventional histological or morphological analysis. Although histological analysis is extremely useful and accurate for diagnosing and staging diseases, such as lung tumors, its procedures are time-consuming and require expertise to interpret the results. This is true in clinical practice. Despite being the most definite assessment of lung cancer grading, histological examination using percutaneous needle biopsy is invasive and the specimen retrieved does not always represent the entire lesion due to sampling errors (18). On the other hand, the use of bioimaging modalities overcomes these obstacles. Compared to conventional single bioimaging modality, such as CT, MRI or ultrasonography, ^{18}F-FDG PET has advantages in the evaluation of malignancies, including diagnosing, staging tumors, evaluating biological characteristics and monitoring tumor progression. Similarly, our results derived from micro-PET corresponded with that of a standard histological analysis. Such findings have great impact on future experimental design, since the use of bioimaging modalities, such as micro-PET, means that histological analysis will not be required at each stage, allowing for serial follow-up and assessment in the last stages of the disease.

Despite the successful demonstration of ^{188}Re-rhk5 delivery to A549 tumor therapy, there are several limitations to the present study. Although ^{188}Re-rhk5 showed a higher tumor uptake and longer retention in A549 tumors, the

absolute tumor uptake value was relatively low, due in part to the hydrophilic character of rhk5 and the small molecular size, leading to a short circulation half-life and rapid kidney clearance. Widespread necrosis was also found in the control groups. This also confirms our previous hypothesis that the lower SUVmax readings exhibited by the control group compared to mice treated only with ^{188}Re-rhk5 were due to a large volume of necrotic cells. Our tumor model was an animal model and the time course of ^{18}F-FDG uptake may be different in humans. In addition, the behavior of ^{18}F-FDG uptake in A549 tumors may not be representative of that in other types of tumors.

Our results indicate that the specific inhibition of A549 tumor growth with ^{188}Re-rhk5 provides an effective novel treatment modality for lung cancer. ^{18}F-FDG PET is a non-invasive imaging tool with which to assess early tumor responses to ^{188}Re-rhk5 therapy. Further improvement of the treatment efficacy is currently in progress.

Acknowledgements

This study was supported by the National Natural Science Foundation of China (NSFC; no. 30570524, 81071181 and 81000622), the Science and Technology Commission of Shanghai Municipality (no. 09431900900), the Shanghai Leading Academic Discipline Project (S30203) and the Medical Engineering (Science) Cross micro-PET Special Foundation of Shanghai Jiaotong University (no. YG08PETZD01).

References

1. Folkman J: Angiogenesis. Annu Rev Med 57: 1-18, 2006.
2. Cao Y, Chen A, An SS, Ji RW, Davidson D and Llinas M: Kringle 5 of plasminogen is a novel inhibitor of endothelial cell growth. J Biol Chem 272: 22924-22928, 1997.
3. Lambert B and de Klerk JM: Clinical applications of ^{188}Re-labelled radiopharmaceuticals for radionuclide therapy. Nucl Med Commun 27: 223-229, 2006.
4. Kaminski MS, Tuck M, Estes J, *et al*: ^{131}I-tositumomab therapy as initial treatment for follicular lymphoma. N Engl J Med 352: 441-449, 2005.
5. Fontanini G, Lucchi M, Vignati S, *et al*: Angiogenesis as a prognostic indicator of survival in non-small cell lung carcinoma: a prospective study. J Natl Cancer Inst 89: 881-886, 1997.
6. Westerterp M, van Westreenen HL, Reitsma JB, *et al*: Esophageal cancer: CT, endoscopic US, and FDG PET for assessment of response to neoadjuvant therapy – systematic review. Radiology 236: 841-851, 2005.
7. Nakamura R, Obara T, Katsuragawa S, *et al*: Failure in presumption of residual disease by quantification of FDG uptake in esophageal squamous cell carcinoma immediately after radiotherapy. Radiat Med 20: 181-186, 2002.
8. Zhang HX, Fang L, Cheng J, Wei Z and Hua ZC: Expression of biologically active kringle 5 domain of human plasminogen in *Escherichia coli*. Prep Biochem Biotechnol 35: 17-27, 2005.
9. Schibli R, Schwarzbach R, Alberto R, *et al*: Steps toward high specific activity labeling of biomolecules for therapeutic application: preparation of precursor [(^{188})Re(H_2O)$_3$(CO)$_3$](+) and synthesis of tailor-made bifunctional ligand systems. Bioconjug Chem 13: 750-756, 2002.
10. Yu J, Hafeli UO, Xia J, *et al*: Radiolabelling of poly(histidine) derivatized biodegradable microspheres with the ^{188}Re tricarbonyl complex [^{188}Re$(CO)_3(H_2O)_3]^+$. Nucl Med Commun 26: 453-458, 2005.
11. Ma Y, Yu J, Han Y, *et al*: Radiolabeling RGD peptide and preliminary biodistribution evaluation in mice bearing S180 tumors. Nucl Med Commun 31: 147-151, 2010.
12. Veitonmaki N, Cao R, Wu LH, *et al*: Endothelial cell surface ATP synthase-triggered caspase-apoptotic pathway is essential for k1-5-induced antiangiogenesis. Cancer Res 64: 3679-3686, 2004.
13. Paganelli G, Bartolomei M, Grana C, Ferrari M, Rocca P and Chinol M: Radioimmunotherapy of brain tumor. Neurol Res 28: 518-522, 2006.
14. Zalutsky MR: Current status of therapy of solid tumors: brain tumor therapy. J Nucl Med 46 (Suppl 1): 151-156, 2005.
15. Reardon DA, Akabani G, Coleman RE, *et al*: Salvage radioimmunotherapy with murine iodine-131-labeled antitenascin monoclonal antibody 81C6 for patients with recurrent primary and metastatic malignant brain tumors: phase II study results. J Clin Oncol 24: 115-122, 2006.
16. Riva P, Franceschi G, Riva N, Casi M, Santimaria M and Adamo M: Role of nuclear medicine in the treatment of malignant gliomas: the locoregional radioimmunotherapy approach. Eur J Nucl Med 27: 601-609, 2000.
17. Dormehl IC, Louw WK, Milner RJ, Kilian E and Schneeweiss FH: Biodistribution and pharmacokinetics of variously sized molecular radiolabelled polyethyleneiminomethyl phosphonic acid as a selective bone seeker for therapy in the normal primate model. Arzneimittelforschung 51: 258-263, 2001.
18. Sun L, Wu H, Pan WM and Guan YS: Positron emission tomography/computed tomography with (18)F-fluorodeoxyglucose identifies tumor growth or thrombosis in the portal vein with hepatocellular carcinoma. World J Gastroenterol 13: 4529-4532, 2007.